Cooperative Effects of Rigor and Cycling Cross-Bridges on Calcium Binding to Troponin C

Marie E. Cantino and Abraham Quintanilla
Department of Physiology and Neurobiology, University of Connecticut, Storrs, Connecticut

ABSTRACT   The effects of rigor and cycling cross-bridges on distributions of calcium (Ca) bound within sarcomeres of rabbit psoas muscle fibers were compared using electron probe x-ray microanalysis. Calcium in the overlap region of rigor fibers, after correction for that bound to thick filaments, was significantly higher than in the I-band at all pCa levels tested between 6.9 and 4.8, but the difference was greatest at pCa 6.9. With addition of MgATP, differences were significant at high levels of activation (pCa 5.6 and 4.9); near and below the threshold for activation, Ca was the same in I-band and overlap regions. Comparison of Ca and mass profiles at the A-I junction showed elevation of Ca extending 55–110 nm (up to three regulatory units) into the I-band. Extraction of TnC-reduced I-band and overlap Ca in rigor fibers at pCa 5.6 to the same levels found in unextracted fibers at pCa 8.9, suggesting that variations reported here reflect changes in Ca bound to troponin C (TnC). Taken together, these observations provide evidence for near-neighbor cooperative effects of both rigor and cycling cross-bridges on Ca^{2+} binding to TnC.

INTRODUCTION

Elevation of myoplasmic-free Ca^{2+} in striated muscle leads to actomyosin interaction and generation of contractile force. As originally envisioned (1,2), this process required only binding of Ca^{2+} to troponin C (TnC) to shift tropomyosin (Tm) from its resting position on the thin filament surface and allow binding of myosin to actin. Activation of contraction has since been shown to depend on cooperative interactions between other myofilament proteins as well and to involve transitions between at least three different states of the thin filament (3). In particular, it is proposed that strong myosin binding, in addition to Ca^{2+} binding, is required to fully turn on the thin filament (see reviews 4–7). Both appear to be essential, but structural evidence suggests that they may act at different points in the activation sequence (8). Binding of Ca^{2+} strengthens interactions between troponin I (TnI) and TnC and weakens interactions of TnI with actin, allowing Tm to more readily shift (or be shifted) to a nonblocking location on the actin surface (9). Myosin cross-bridge attachment to actin is likely to exert direct effects on Tm, either by shifting it to its fully open position or by keeping it there once it has moved. However, the binding of myosin to actin can also modulate Ca^{2+} binding to TnC (10,11). There is evidence for both of these mechanisms, but the importance of their effects in different muscle types and with different types of cross-bridge attachment is still in question. Furthermore, these effects will depend on whether they act within a single regulatory unit (seven actins, one Tn, and one Tm) or extend to neighboring units.

Evidence for enhancement of Ca^{2+} binding to TnC by rigor cross-bridge attachment to actin has been demonstrated by previous studies that measured $^{45}Ca^{2+}$ binding in vitro in both skinned skeletal and cardiac muscle (10–16) and changes in TnC structure (17). In contrast, studies investigating effects of cycling cross-bridges on TnC have yielded mixed results. Several studies indicate that cycling cross-bridges or force enhance $^{45}Ca^{2+}$ binding to TnC in skinned cardiac muscle (18,19) but not in skinned skeletal muscle (20–22). Fluorescently labeled TnC has also been used to study TnC structural changes that reflect Ca^{2+} binding. Early results comparing activated fibers at different sarcomere lengths suggested that cycling cross-bridges strongly affect TnC structure (23–25), but later studies employing cross-bridge inhibitors or sarcomere length increases to reduce cross-bridge interaction have not supported this view (17,26, 27). Consistent with the later studies are measurements showing sarcomere length invariance of TnC Ca^{2+} affinity using caged Ca^{2+} compounds and Ca^{2+} fluorophors (28). In contrast, some studies have supported cycling cross-bridge-induced changes in TnC affinity for Ca^{2+} by showing changes in myoplasmic-free Ca^{2+} during contraction in intact and skinned fibers (29–31). In these reports, interventions that reduce interaction of cycling cross-bridges with actin were shown to cause a transient rise of Ca^{2+} in the myoplasm, consistent with a release of Ca^{2+} from TnC.

Thus, questions about the extent to which cycling cross-bridges affect Ca binding to the thin filament persist. All of these studies measured average behavior of large numbers of sarcomeres in whole fibers or fibers segments. Sarcomere inhomogeneity or changes in Ca^{2+} binding elsewhere besides the overlap region could give rise to some of the inconsistencies between methods and results. Moreover, none of these techniques provides direct measurements of

the spatial extent of effects of either cycling or rigor cross-bridges on calcium binding to troponin. A number of reports suggest that effects of cross-bridges on the state of the thin filament extend some distance along the thin filament (e.g., 32–34). Recent studies show that cooperative Ca^{2+} binding to cardiac TnC in isolated filaments requires more than one regulatory unit (35), but the nature and extent of these effects in the intact sarcomere are not clear.

Direct measurements of Ca within individual sarcomeres were first made using autoradiography (36) but with limited spatial resolution. Electron probe x-ray microanalysis (EPXMA) was later shown to be capable of detecting Ca bound to thin filaments (37) and of measuring variations in Ca as a function of position along the thin filaments (38–40). Calcium was shown to be elevated in regions of rigor cross-bridge attachment in rabbit psoas fibers (38), consistent with effects of rigor cross-bridge attachment on Ca^{2+} binding to N-terminal sites on troponin, but this study did not investigate the effects of cycling cross-bridges. Furthermore, effects of rigor cross-bridges between pCa 9.05 and 6.25 were not studied. Here we compare subsarcomere Ca distributions measured in filaments exposed to solutions with and without ATP. Results support effects of both rigor and cycling cross-bridges on Ca^{2+} bound to TnC and extending beyond a single regulatory unit. Calcium distributions at pCa 6.9 raise the possibility that Ca^{2+} binding to C-terminal sites on troponin are also affected by rigor cross-bridge attachment.

METHODS

Fiber dissection, freezing, and cryomicrotomy

Preparation of frozen samples was similar to that described previously (39) and is summarized here. All animal procedures were approved by the University of Connecticut Institutional Animal Care and Use Committee. Bundles of psoas fibers were dissected from New Zealand white rabbits immediately after euthanasia (Na Pentobarbital, IV, 100 mg/kg) and skinned for 45 min in 0.5% Brij 58 in relaxing solution (see below) plus 2 mM dithiothreotol (DTT) and 0.1 mM leupeptin. After skinning, fibers were stirred on ice overnight in relaxing solution with DTT and leupeptin. They were then stored in a fresh change of this solution mixed 1:1 with glycerol at $-17°C$. For each experiment, strips of ~10 fibers were isolated, skinned again in relaxing solution plus 1% Triton X 100 on ice for 15–20 min with agitation, then attached to a force transducer (photoelectric displacement measuring device modified after Chui (41) and transilluminated with a laser). Once attached to the apparatus, the fiber bundles were immersed in a series of Plexiglas wells containing bathing solutions (42) at ambient temperature (23–25°C). Fibers were stretched in relaxing solution to sarcomere lengths between 2.8 and 3.2 μm, as measured by laser diffraction. Once stretched, fibers were transferred to low free Ca^{2+} (pCa 8.9–9.0) solution for 15 to 20 min, then to a final buffered Ca^{2+} solution for a minimum of 1 min with agitation to facilitate diffusion. For freezing, the fibers were lifted from the bath and clamped with copper clad pliers cooled to liquid nitrogen temperature. Time between removal from the bath and freezing was ~5 s. Frozen fibers were stored in liquid nitrogen until they were cryosectioned on glass knives at $-122°C$ in either an RMC MT7/CR-21 or a Leica (Wetzlar, Germany) UCT/EMFCS cryoultramicrotome system. Methods for preparing and freeze-drying sections were as described previously (39).

Solution composition

A modified Tyrodes solution used to irrigate fibers during isolation from the rabbit contained 1.5 mM $MgCl_2$, 0.34 mM NaH_2PO_4, 25 mM $NaHCO_3$, 112 mM NaCl, 6 mM KCl, and 2.5 mM $CaCl_2$. Except as noted at the end of this section, fiber bundles were prepared and frozen in solutions composed as follows. Relaxing solution contained 6.66 mM MgAc, 5.8 mM Na_2ATP, 10 mM Na_2CP, 20 mM 3-(N-morpholino)propanesulfonic acid (MOPS), 15 mM K_2EGTA, and 72 mM Kpropionate at pH 7. For skinning and storage this solution was modified with Brij 58, Triton-X100, DTT, and/or leupeptin as described above. Calcium-buffered solutions containing defined levels of free Ca^{2+}, but without ATP (designated ''rigor'' or ''R''), were prepared as described previously (39) and using a computer program (43) to calculate free Ca^{2+} concentrations. Total Ca in rigor solutions was 28–36 μM, whereas Na_2EGTA was varied from 0–13 mM. Actual total Ca was determined by atomic absorption spectroscopy and reported pCa values were adjusted accordingly. The free Mg^{2+} was 1 mM, MOPS was varied (185–255 mM) to keep ionic strength between 144 and 153, and total sodium ranged from 112–139 mM. Final pH was adjusted to 7.0.

A subset of rigor fibers included in this study (six of 30) was prepared using slightly different solution recipes (39). Relaxing solution used for dissection contained 9 mM $MgCl_2$, 4 mM Na_2ATP, 10 mM MOPS, 5 mM K_2EGTA, 100 mM Kpropionate, and 0.5% Brij 58 was used for skinning. Calcium-buffered solutions were similar in composition to those described above but had lower ionic strength (120–131 mM). Calcium levels measured by EPXMA did not differ significantly from later fibers, and the sets have been pooled.

For investigating effects of cycling cross-bridges, Ca^{2+}-buffered solutions (designated ''A'' and prepared using the later protocol) included 5 mM MgATP and 10 mM Na_2 creatine phosphate. Creatine phosphokinase (CPK) up to 248 units/ml was added in some experiments but did not significantly affect subsarcomere Ca distributions measured by EPXMA. Ionic strength was 177–180, MOPS was 60 mM, total Na was 155 mM, free Mg^{2+} was 1 mM, and total Ca was 35–38 μM.

TnC extraction and SDS-PAGE

Before freezing, TnC was extracted from some fiber bundles by incubation for 50 min on ice in a solution containing 20 mM MOPS, 5 mM Na_2EDTA, 0.5 mM trifluoperazine, and 150 mM Kpropionate. The extent of extraction was assessed by sodium dodecyl sulfate-polyacrylamide gel electrophoresis (SDS-PAGE) (modified from Laemmli (44)) carried out on similarly prepared fibers.

Spectral collection and processing

The EPXMA methods used were similar to those described previously (39,40). Data were collected at room temperature in scanning transmission (STEM) mode using an EM 910 electron microscope (Carl Zeiss SMT, Oberkochen, Germany) equipped with an LaB6 gun, a 30-mm² Be window detector, and an ExL2 analytical system (Oxford Instruments, Oxon, UK).

Two modes of data collection were used. In ''raster'' mode, the beam was scanned in a rectangular raster (typically 0.2 × 1.0 μm; see Fig. 1 a) for 500–1000 s. Raster data consisted of sets of spectra collected sequentially in three regions (nonoverlap A-band = H, I-band = I, and overlap = O) of each half sarcomere and a fourth spectrum over the support film to estimate both Ca and mass (bremsstrahlung (brem)) contributed by the support. Four to six half sarcomeres were sampled in each of 4–6 different fibers. Beam current was monitored for constancy over the period required to collect data from a half sarcomere. In ''digital image'' mode, the position of the focused beam was controlled by a processor, which scanned it sequentially through a 128 × 128 array of points. Since the long acquisition times were a practical limitation on the number of samples analyzed using image mode, we used raster data to first assess sample to sample variations. We then selected
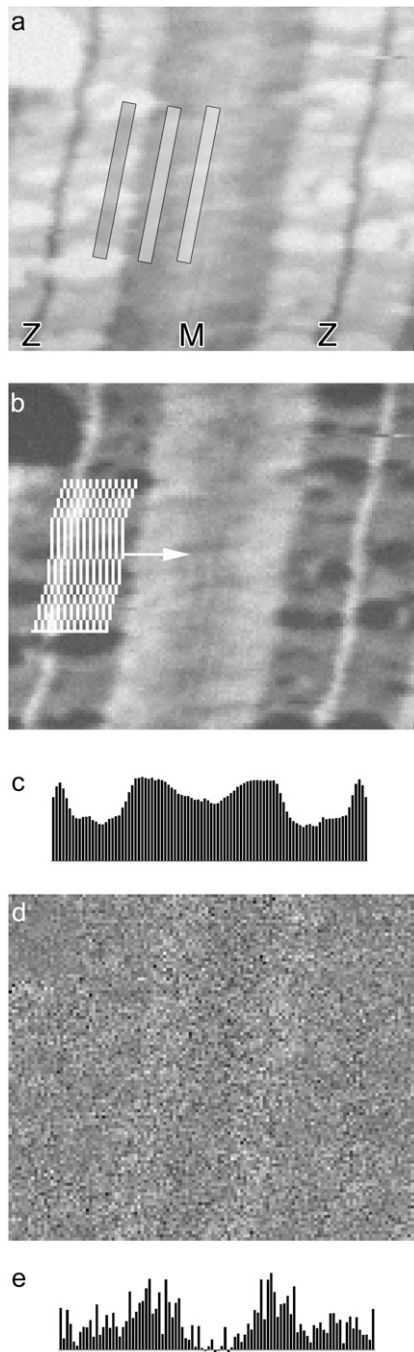
FIGURE 1 Data acquisition strategy. See text for details. (*a*) STEM image with rectangles illustrating positions of rasters used to collect data from I, O, and H regions. Z = Z-band, M = M-band. (*b*) Brem image with masks at successive positions. Note that contrast is reversed for x-ray images. (*c*) Brem profile obtained from brem image and masks in panel *b*. (*d*) Calcium image. (*e*) Ca profile obtained by applying masks in *b* to Ca image in *d*.

representative samples for each condition from which to collect digital images to obtain the high resolution data included here.

Spectra acquired in both raster and image modes were processed and quantified using a digital top-hat filter and linear least squares fitting routine. For quantification of raster data, Ca concentration ([Ca]) in H, I, and O

regions was computed using the Hall method (45) with absolute quantification achieved via protein and binary standards (46) and corrections for the average atomic number of the sample. This method normalizes the Ca x-ray count, which is a measure of the number of Ca atoms, to the brem x-ray signal, which is a measure of the total dry mass of the irradiated volume, to derive a concentration in mmoles/kg dry wt. The Ca concentration for the thin filaments alone in the overlap region, $[Ca]_{Io}$, was estimated from the Ca concentration measured in the I-band ($[Ca]_I$), and the Ca count measured in the I ($Cact_I$), O ($Cact_O$), and H regions ($Cact_H$) of the same half sarcomeres, as shown in the equation below:

$$[Ca]_{Io} = [Ca]_I \times (Cact_o - Cact_H)/Cact_I.$$

As discussed previously (38), differences in filament density in the two regions may result in an underestimation of $[Ca]_{Io}$ by not more than ~10%.

Image data were treated as described previously (39,40) and summarized here. At each pixel, Ca and brem counts were quantified as described above. Profiles corresponding to Ca and brem distributions along A- and I-bands in each sarcomere were then generated from these images as summarized in Fig. 1. A mask was drawn to follow the A-I junction (Fig. 1 *b*) using the STEM or brem image as a guide. The sum of pixel counts within the mask was computed at each successive position as the mask was moved along the sarcomere in the direction shown to generate Ca count and brem count profiles (Fig. 1, *c* and *e*). Pixels associated with remnants of the sarcoplasmic reticulum (identified by their high P concentration) were removed from these sums, and corrections were made for Ca and brem counts associated with the support film. To improve counting statistics and assess sarcomere to sarcomere variation, data from three to six half sarcomeres were combined after normalizing counts in each profile to the average brem (mass) counts over the entire half sarcomere, thereby correcting for image to image variations in mass thickness and electron dose. The resulting means and standard errors of normalized counts from different half sarcomeres were plotted as a function of position in the half sarcomere (*gray bars* in Figs. 3, 4 and 5 *b*). The average normalized Ca count measured in the H-zone, just outside the M-band, was then used to estimate Ca^{2+} bound to myosin. A scaling factor for this correction was based on the change in brem counts, ranging from one at the center of the overlap to zero in the I-band and applied to the Ca profile (designated ''H Corr Ca'' and shown as *black bars* in Fig. 3). To facilitate comparison of the change in Ca and mass at the A-I junction (Fig. 4), individual values in profiles of H Corr Ca and brem were each scaled to their maximum value, as estimated from an average of the highest four consecutive pixel values in the overlap region.

RESULTS

Ca data from raster analysis

Distributions of Ca measured in raster mode of fibers frozen in solutions without and with MgATP are shown in Fig. 2, *a* and *b*. The lower three curves in each panel show the Ca concentration (in mmoles/kg dry wt) measured in I, O, and H regions (illustrated in the half sarcomere cartoon in Fig. 2 *c*). The uppermost curves represent $[Ca]_{Io}$, our estimate of the [Ca] bound to thin filaments in the overlap region (calculated from the other three measurements as described in Methods). Fibers were sampled at five pCa levels without and with ATP, plus an additional data set collected for rigor fibers at pCa 4.5 to confirm that myofilament Ca levels had reached maximum.

The data show prominent differences in the absence and presence of ATP. In rigor fibers (Fig. 2 *a*), the mean $[Ca]_{Io}$ was higher than $[Ca]_I$ at all pCa levels measured below 8.9,
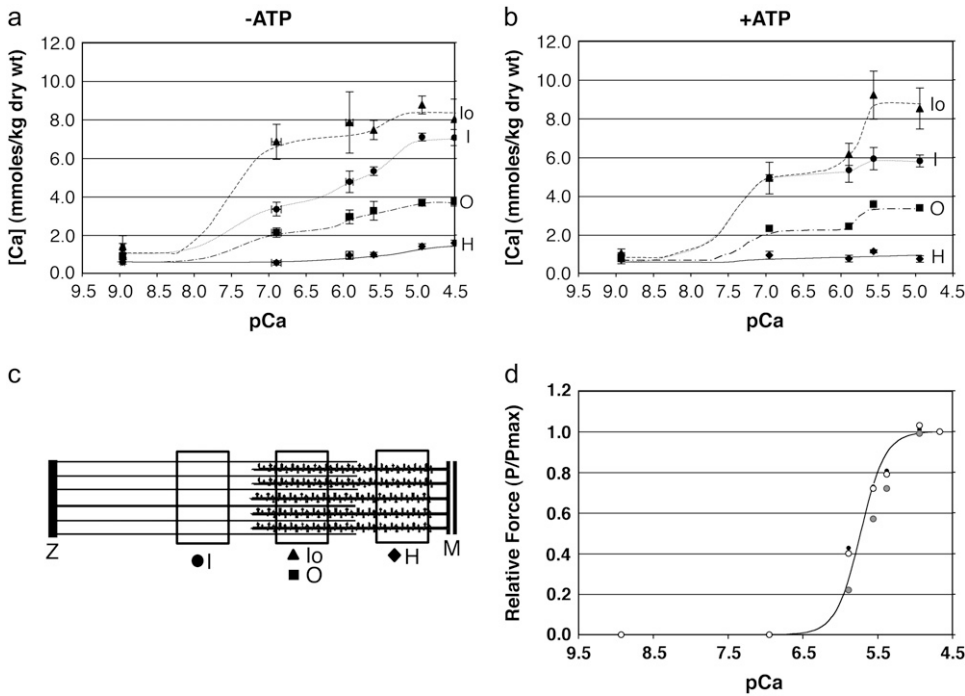
FIGURE 2 (*a*. and *b*) Ca distributions measured in raster mode collected in H, I, O, and Io regions. Points represent mean ± SE for $N = 4$–6 fibers, with 4–6 sarcomeres sampled per fiber. (*c*) Cartoon illustrating regions used for raster mode. (*d*) Relative force as a function of pCa. Force measurements are from three bundles, as denoted by different symbols.

with the greatest difference at pCa 6.9 and diminishing at higher free Ca^{2+}. In the presence of MgATP, $[Ca]_{Io}$ was nearly equal to $[Ca]_I$ at pCa 6.9 and 5.9 but was significantly greater at 5.6 and 4.9 ($P < .05$, Student's *t*-test). The $[Ca]_I$ increased only minimally from 6.9 to 4.9.

We also measured the force-pCa relationship for three additional fibers using the same solutions (plus one additional solution at pCa 5.4). Data are plotted in Fig. 2 *d* as relative force (P/Pmax) versus pCa. The rise in force appears to be correlated with the second rise in Ca bound to the thin filament between pCa 5.9 and 5.6. Force was undetectable at pCa 6.9.

Ca profiles from x-ray images

Data from digital images are shown in Fig. 3. These profiles, each of which includes data from 3–6 half sarcomeres in a single fiber, show high resolution Ca-binding distributions from Z- to M-band and oriented as shown in the cartoon. At pCa 8.9, where little or no Ca is expected to be bound either to thin or thick filaments, the distribution is low throughout the sarcomere. As observed with raster mode, Ca binding is enhanced in the overlap region at pCa 7.0 and 5.9 in rigor (*left*) but not with ATP (*right*). On the other hand, increased Ca in the overlap is observed both with and without ATP at pCa 5.6 and 4.9. Profiles also show that after the decline associated with the A-I junction, calcium binding is relatively uniform for most of the I-band, though sometimes declining very gradually toward the Z-band. The steeper decline in Ca at the far left of profiles with high I-band Ca suggests that less Ca binds to thin filaments in the Z-band,

but this feature was variable and may depend on how well aligned profiles were in this area. Since data sets combined for these profiles were aligned at the A-I junction, slight variations in sarcomere length resulted in poor alignment at the Z-band.

To determine whether cooperative effects of cross-bridges on Ca^{2+} binding to troponin extended beyond the region of actomyosin interaction, we compared normalized Ca profiles with associated brem (mass) profiles (Fig. 4). Both profiles are displayed on the same plots to facilitate comparison, and all points in each profile are scaled to an average of the highest four pixels for that profile. The Ca begins to fall 2–4 pixels further into the I-band than the drop in the mass distribution, corresponding to distances of ~55–110 nm.

Ca in TnC-extracted fibers

To determine how much of the Ca detected by EPXMA in the I and Io regions is bound to TnC, we carried out analysis of fibers from which TnC had been extracted (Fig. 5). Calcium concentration in H, I, and Io regions are shown in Fig. 5 *a* for TnC-extracted fibers frozen in pCa 5.6R solution. Data from unextracted fibers at pCa 9.0R and 5.6R (also included in Fig. 2) are shown for comparison. Extraction of TnC resulted in reduction of $[Ca]_I$ and $[Ca]_{Io}$ at 5.6R to levels comparable to those at pCa 9.0R. Fig. 5 *b* shows a Ca profile from a TnC-extracted fiber, showing that Ca binding is low and relatively uniform throughout the I-band and overlap regions. After correction of the overlap region for the H-zone Ca (*black bars*), there is no indication of Ca-binding enhancement in the overlap region. Similar results were obtained in
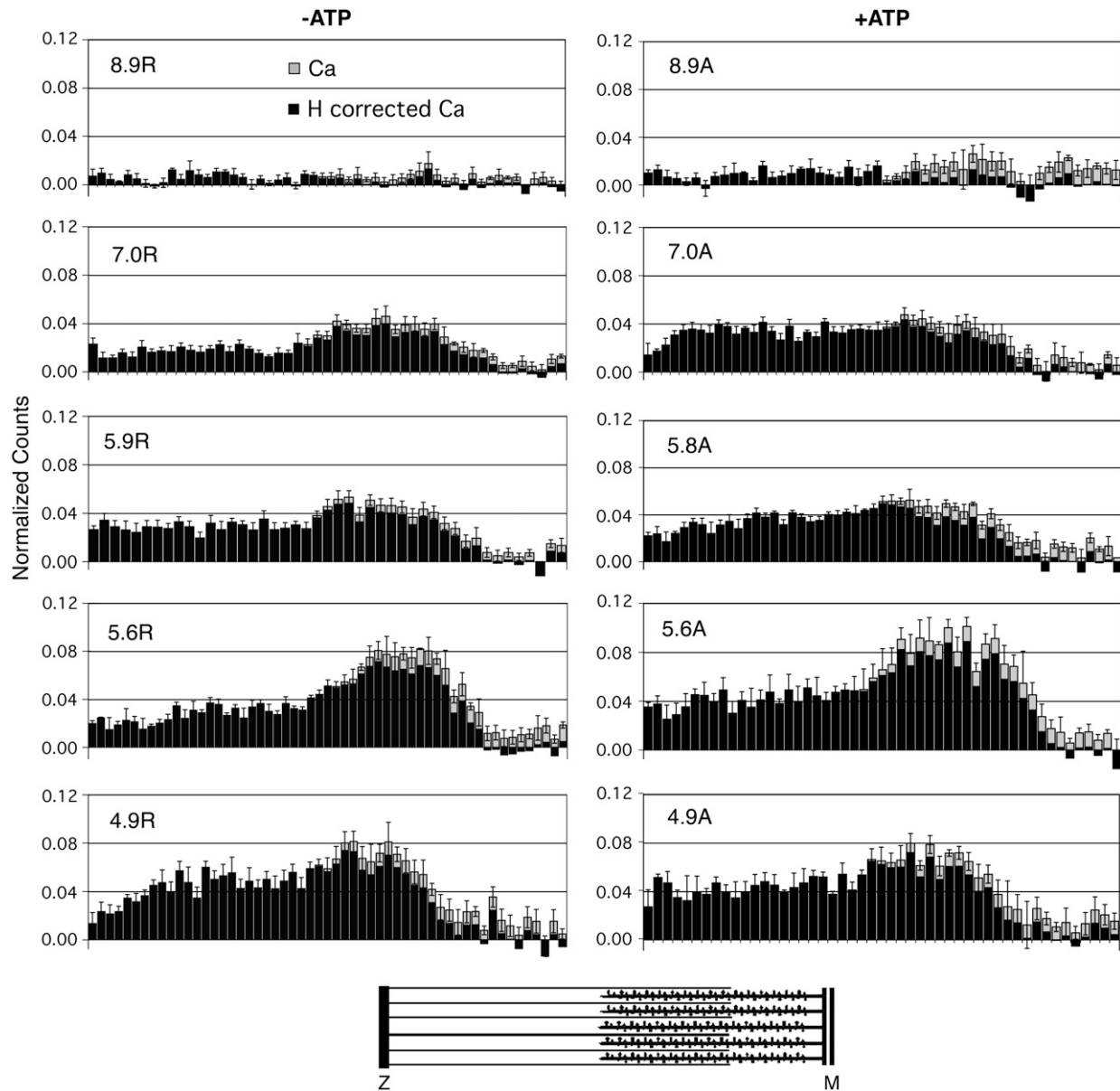
FIGURE 3   Half sarcomere Ca profiles from digital x-ray images. Profiles are oriented as shown in the cartoon below. The black portion of each bar (H corr Ca) shows normalized Ca level counts after subtraction of the Ca associated with thick filaments, based on H-zone Ca (see text for details). Error bars are mean ± SE for $N = 4$–6 half-sarcomeres. Label in upper left corner of each profile indicates the pCa and whether ATP was present (*A*) or absent (*R*) in the bathing solution.

extracted fibers in pCa 6.9A solutions (data not shown). Extraction of TnC was verified by SDS gel electrophoresis (Fig. 5 *c*).

DISCUSSION

In this study we set out to compare effects of rigor and cycling cross-bridges on binding of Ca^{2+} to TnC. Our results show changes in subsarcomere Ca distributions that are consistent with enhancement of Ca^{2+} binding to TnC by both rigor and cycling cross-bridges and extending for a distance of one and a half to three regulatory units. Results

also suggest effects of rigor cross-bridges on both N-terminal and C-terminal sites of TnC.

Cross-bridge effects on Ca^{2+} binding to troponin

The average value of $[Ca]_{Io}$ measured in rigor and activated fibers at pCa 4.9 and 4.5 (Fig. 2 *a*) was 8.4 mmoles/kg dry wt. Subtraction of the $[Ca]_{Io}$ measured at pCa 8.9 gives an average change of 7.0 mmoles/kg dry wt. The expected value for four Ca^{2+} bound per troponin is around 6.8 mmoles/kg dry wt, assuming that the I-band includes thin filaments consisting of actin, Tn, and nebulin, as well as titin filaments
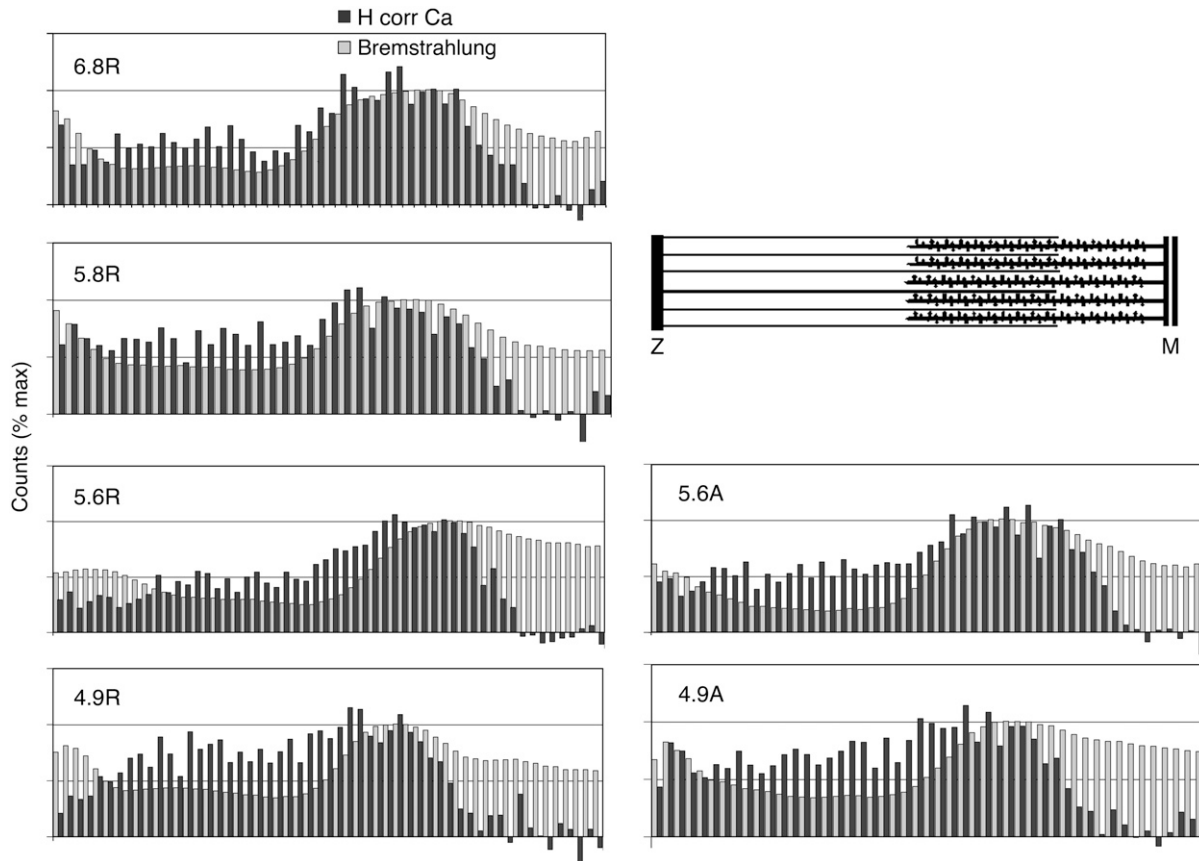
FIGURE 4 Comparison of Ca and brem (mass) profiles for maps shown in Fig. 3. Black bars are H corr Ca (as in Fig. 3) and gray bars show brem at the same position. Individual values within each profile are normalized to the maximum in the overlap for that profile. Profiles are oriented as shown in the cartoon, with the bulge in the brem profile indicating the position of the overlap region.

that are elastic in the I-band (47). It therefore seems likely that the maximum values we measure in $[Ca]_{Io}$ correspond to saturation of TnC binding sites for Ca^{2+}.

Our measurements of subsarcomere calcium distributions in rigor fibers at pCa 5.9 and lower (higher free Ca^{2+}) are

largely consistent with previous findings with EPXMA and other techniques. All previous studies appear to agree that rigor cross-bridge attachment increases Ca^{2+} binding to troponin, and this conclusion is also supported by our data. Not only did both raster and image data show higher $[Ca]_{Io}$
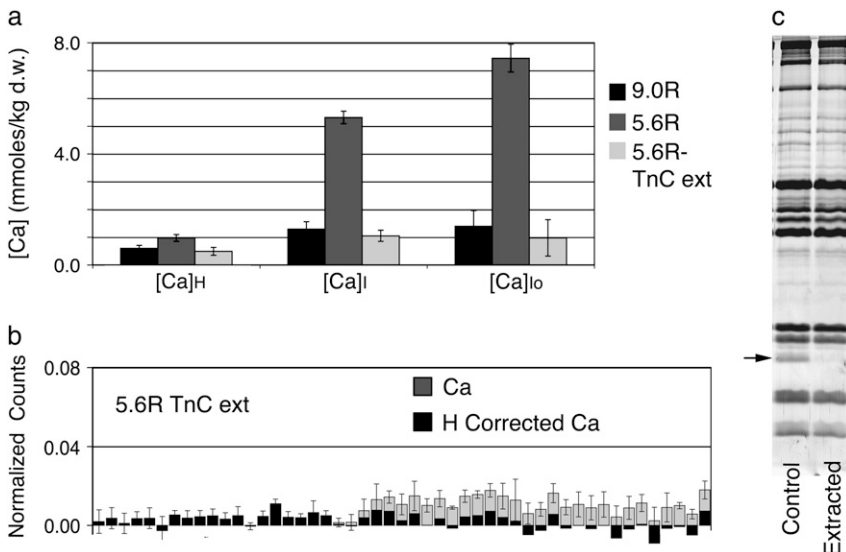

FIGURE 5 Calcium in TnC-extracted fibers. (*a*) Raster data from extracted fibers in pCa 5.6R solution; included for comparison are values from Fig. 2 for unextracted fibers in pCa 9.0R and 5.6R solutions. (*b*) X-ray image profile for TnC-extracted fiber frozen in pCa 5.6R solution. Compare to profile for control fibers in the same solution in Fig. 3. (*c*) Gels showing extent of TnC extraction. Arrow shows position of TnC band.

compared with $[Ca]_I$, but when TnC was extracted, measured Ca in the I and Io regions dropped to pCa 8.9 levels and Ca enhancement in the Io region was lost. Our results at pCa 6.9 suggest that the Ca^{2+} affinity of the C-terminal sites may also be affected by rigor cross-bridge attachment. Effects of rigor cross-bridges on Ca binding at pCa 6.9 were not reported in previous studies of skeletal muscle using $^{45}Ca^{2+}$ (12,13,48), but the lower free Mg^{2+} used in this study may account for this difference (see discussion below).

A second conclusion of previous measurements with $^{45}Ca^{2+}$ and EPXMA was that rigor cross-bridges increase Ca^{2+} binding to Tn even at saturating levels of free Ca^{2+} (12–14,38). This suggests either that rigor cross-bridge attachment is a requirement for Ca^{2+} binding to one of the two N-terminal Ca-binding loops on TnC or that the affinity shifts by several orders of magnitude. Our study was inconclusive on this point: significant Ca enhancement by rigor cross-bridges persisted at pCa 4.9, but the difference was diminished at pCa 4.5 and was not statistically significant.

Patterns of myofilament Ca binding in fibers frozen in the presence of ATP differed from those found in rigor fibers. Below the threshold for activation (pCa 6.9) and at low levels of activation (pCa 5.9), there was no significant difference between I and Io values. However, at higher activation (pCa 5.6) the $[Ca]_{Io}$ was significantly higher than $[Ca]_I$ ($P < .05$, Student's t-test), and the difference in means was greater than in rigor. This difference between [Ca] in I and Io regions persisted even when force was at maximal levels (pCa 4.9). Similar results were found in normalized Ca count profiles from digital images.

This result is consistent with aequorin and Fura 2 studies, which support a drop in TnC affinity for Ca^{2+} caused by detachment of cycling cross-bridges (29–31,49), but differs from conclusions of studies with ^{45}Ca and fluorescently labeled TnC, which found no effect of cycling cross-bridges on Ca levels (20,21) or TnC structure (17,26) in skeletal muscle. This is puzzling, since our results and conclusions for rigor fibers are largely consistent with their findings. We can only speculate that differences in the parameters measured with each method lead to these differences in results for cycling cross-bridges.

In EPXMA studies, effects of cycling cross-bridges on Ca binding are measured by comparing different regions within a relatively small number of sarcomeres selected for length (2.8–3.2 μm) and alignment. Both $^{45}Ca^{2+}$ and fluorescent labeling studies compare $^{45}Ca^{2+}$ binding or fluorescence signals that represent behavior of all sarcomeres within a fiber, fiber segment, or fiber bundle. Whole fiber measurements provide a more accurate indication of average Ca binding in a fiber, but interpretation may be complicated by sarcomere inhomogeneity (skew and/or sarcomere length variations), which are most pronounced in activated fibers and especially at high levels of activation. These effects produce variations in the amount of filament overlap that may obscure cross-bridge-dependent differences in total cal-

cium or fluorescence. Furthermore, effects of cross-bridges on Ca^{2+} binding to TnC in whole fiber measurements are inferred by making changes in sarcomere length or addition of cross-bridge inhibitors with the assumption that changes occur in the overlap region of the thin filament. Our measurements suggest that changes in cross-bridge binding may affect Ca in both I-band and overlap regions. The nature and cause of this difference is unclear (see discussion below) but would further complicate interpretation of average behavior. By comparing Ca binding in the presence and absence of cross-bridges within the same sarcomeres, EPXMA may resolve differences not detected by other techniques, as has been suggested to reconcile studies of fluorescent TnC with Ca^{2+} dye studies (26).

Another methodological difference is the use of fiber bundles for EPXMA, compared with single fibers used in most other studies. The greater diffusion distances in bundles might create ATP gradients and an increase in rigor-like cross-bridge attachments at the center of our samples. We cannot completely rule this out, but two factors lead us to conclude that ATP depletion is not a major source of error in our results. First, the majority of our data are collected from the outermost fiber because areas near the surface have the least damage due to ice crystal formation. We have also looked for correlations between Ca enhancement and the degree of ice crystal damage and have found none. Since freeze damage generally correlates with fiber depth, this suggests that depth within the fiber is not a major factor in our results. Nor did we find any effect of varying CPK concentration from 0 to 248 units/ml at pCa 5.6 and 4.9.

The three-state activation model requires that the thin filament change from a "blocked" to a "closed" and ultimately to an "open" conformation as described by McKillop and Geeves (3). Cooperative effects of cross-bridges could result either from direct effects on Tm in the closed to open transition or indirectly by increasing Ca binding to troponin, which promotes the blocked to closed transition or both. Our observation of increased [Ca] in the overlap region of activated thin filaments provides support for indirect effects under some conditions but does not exclude direct effects as well. It is also possible that increased binding of Ca to TnC in the overlap region is a consequence rather than a cause of increased thin filament activation. Recent studies using TnC mutants that are site-I inactive (50) suggest that at higher levels of Ca^{2+}, the level of activation is determined by cross-bridges rather than Ca^{2+}, in which case the Ca distributions we measure may indicate variations in the state of the thin filament as a function of position.

Spatial extent of cross-bridge effects on Ca^{2+} binding

In a previous study of Ca distributions in rigor fibers (38) we concluded that effects of rigor cross-bridges could not extend more than 150 nm or ~4 regulatory units, but we were

limited by the width of masks used to generate Ca profiles. Here masks were only one pixel wide (26–30 nm, depending on the image), and comparison of mass and Ca profiles at the A-I junction shows a shift of two to four pixels between the profiles that suggests Ca^{2+}-binding enhancement extending for one and a half to three regulatory units for both rigor and cycling cross-bridges. This result is consistent with other estimates based on myosin S1 binding (32,33) and the spread of activation from a functional Tn (34). Profiles in Fig. 4 suggest that this spread may be greater at higher Ca^{2+}, but more detailed modeling of a larger number of profiles is needed to determine what parameters affect this relationship.

Ca^{2+} binding at pCa 6.9

Our previous studies did not investigate Ca distributions at pCa levels between 6.2 and 9.0. In this study, we see significant differences between $[Ca]_I$ and $[Ca]_{Io}$ at pCa 6.9. Using the curves in Fig. 2, *a* and *b*, and assuming that the maximum Ca estimated for the Io region represents saturation of the four binding sites on TnC, it appears that in rigor at pCa 6.9, I-band, and Io sites are ~30% and 80% occupied, respectively, implying saturation of all of the C-terminal sites on TnC and at least one of the regulatory (N-terminal) sites in the overlap region. Therefore, it seems likely that rigor cross-bridge attachment increases Ca^{2+} binding to C-terminal sites as well as N-terminal sites on TnC. When MgATP is included in the bath, both values are ~50% of maximum. The drop in $[Ca]_{Io}$ is not unexpected; if strongly bound cross-bridges increase Ca^{2+} binding to C-terminal sites on troponin, then addition of ATP below the threshold for force will abolish rigor cross-bridge attachment. The reason for the higher level of $[Ca]_I$ with ATP is not clear. It may be that in the absence of ATP, rigor force exerted on the thin filament decreases affinity of C-terminal sites in the nonoverlap thin filament, resulting in lower $[Ca]_I$. Thin filament structural changes during isometric contraction have been documented using x-ray diffraction (51,52). Structural changes are likely to be greatest in the nonoverlap region of the thin filament, and recent results suggest that strong cross-bridge attachment and tension may exert separate effects on filament structure (53). We previously reported that treatment of activated fibers with butanedione monoxime reduced enhancement of calcium in the overlap region (54), and subsequent analysis (M. E. Cantino and A. Quintanilla, unpublished data) has indicated that this reflects mainly an increase in $[Ca]_I$, rather than a decrease in $[Ca]_{Io}$, consistent with effects of thin filament tension on Ca binding to troponin in the I band.

Studies using $^{45}Ca^{2+}$ detected less Ca^{2+} binding at around pCa 6.9 than found here, probably reflecting differences in free Mg^{2+} levels used in bathing solutions. In $^{45}Ca^{2+}$ studies, free Mg^{2+} was 5 mM (12,13,48) compared with 1 mM in our investigation. Other studies show that $^{45}Ca^{2+}$ measured in fibers at pCa 7.0 increases substantially when free Mg^{2+} is decreased from 10 to 1 mM in skeletal muscle (48)

or to 2 mM in cardiac muscle (16). This can be accounted for by changes in the cation occupancy of C-terminal (Ca^{2+}-Mg^{2+} binding) sites on TnC (16).

It is not clear what role, if any, cross-bridge- or tension-mediated effects on Ca^{2+} binding to the C-terminal sites might play in vivo. Binding of either Mg^{2+} or Ca^{2+} to these sites is thought to stabilize TnC-TnI interactions and binding of TnC to the thin filament (55). Structural studies suggest some differences in the Mg^{2+}- and Ca^{2+}-loaded structures in cardiac muscle (56), and altered signaling in this area has been linked to familial hypertrophic cardiomyopathy (57). It is also possible that if Ca^{2+} affinity of C-terminal sites in the I-band is reduced sufficiently by tension or myosin binding early in activation, this could increase Ca^{2+} available for binding to N-terminal sites.

Binding of Ca^{2+} to myosin light chains and titin

The $[Ca]_{Io}$ curves (Fig. 2, *a* and *b*) and H corr Ca profiles (Figs. 3 and 4) represent our best estimate of Ca levels after correction for Ca bound to the cross-bridge regions of the thick filament. We assume that these corrected values represent primarily Ca^{2+} binding to troponin. However, there are several possible pitfalls to this interpretation. First, we assume that thick filament bound Ca is the same in the H-zone and in the overlap region. Our previous data from overstretched frog semitendinosus fibers (39) showed relatively uniform Ca distributions along the thick filament but did not rule out the possibility that cross-bridge attachment increases affinity of myosin light chains for Ca^{2+}. Our results here showing uniformly low Ca distributions in TnC-extracted fibers suggest otherwise but do not completely exclude the possibility that Ca binding to myosin light chains is increased by cross-bridges only when TnC is present.

Calcium binding to the PEVK region of titin has been supported by recent studies (58,59). Based on the known location of the PEVK region, this is unlikely to be the source of extra Ca we measure in the overlap region, and uniformity of Ca distributions in TnC-extracted fibers also appears to rule this out. It should be noted, however, that our results do not rule out Ca^{2+} binding to titin. At the sarcomere lengths used here, the PEVK region is likely to be highly stretched, distributing the Ca over a large enough region of the I-band to make it difficult to detect.

REFERENCES

1. Haselgrove, J. C. 1972. X-ray evidence for a conformational change in the actin containing filaments of vertebrate striated muscle. *Cold Spring Harb. Symp. Quant. Biol.* 37:341–352.

2. Parry, D. A., and J. M. Squire. 1973. The structural role of tropomyosin in muscle regulation: analysis of the x-ray diffraction patterns from relaxed and contracting muscles. *J. Mol. Biol.* 75:33–55.

3. McKillop, D. F. A., and M. A. Geeves. 1993. Regulation of the interaction between actin and myosin subfragment 1: evidence for three states of the thin filament. *Biophys. J.* 65:693–701.

4. Gordon, A. M., E. Homsher, and M. Regnier. 2000. Regulation of contraction in striated muscle. *Physiol. Rev.* 80:853–924.

5. Lehrer, S. S., and M. A. Geeves. 1998. The muscle thin filament as a classical cooperative/allosteric regulatory system. *J. Mol. Biol.* 277:1081–1089.

6. Squire, J. M., and E. P. Morris. 1998. A new look at thin filament regulation in vertebrate skeletal muscle. *FASEB J.* 12:761–771.

7. Tobacman, L. S. 1996. Thin filament-mediated regulation of cardiac contraction. *Annu. Rev. Physiol.* 58:447–481.

8. Pirani, A., M. V. Vinogradova, P. M. G. Curmi, W. A. King, R. J. Fletterick, R. Craig, L. S. Tobacman, C. Xu, V. Hatch, and W. Lehman. 2006. An atomic model of the thin filament in the relaxed and Ca2+-activated states. *J. Mol. Biol.* 357:707–717.

9. Lehman, W., P. Vilbert, P. Uman, and R. Craig. 1995. Steric blocking by tropomyosin visualized in relaxed vertebrate thin filaments. *J. Mol. Biol.* 251:191–196.

10. Bremel, R. D., and A. Weber. 1972. Cooperation within actin filament in vertebrate skeletal muscle. *Nature.* 238:97–101.

11. Bremel, R. D., J. M. Murray, and A. Weber. 1972. Manifestations of cooperative behavior in the regulated actin filament during actin-activated ATP hydrolysis in the presence of calcium. *Cold Spring Harb. Symp. Quant. Biol.* 37:267–275.

12. Fuchs, F. 1977. The binding of calcium to glycerinated muscle fibers in rigor, the effect of filament overlap. *Biochim. Biophys. Acta.* 491:523–531.

13. Fuchs, F. 1977. Cooperative interactions between calcium-binding sites on glycerinated muscle fibers. The influence of cross-bridge attachment. *Biochim. Biophys. Acta.* 462:314–322.

14. Fuchs, F. 1978. On the relation between filament overlap and the number of calcium binding sites on glycerinated muscle fibers. *Biophys. J.* 21:273–276.

15. Hofmann, P. A., and F. Fuchs. 1987. Effect of length and cross-bridge attachment on Ca2+ binding to cardiac troponin C. *Am. J. Physiol.* 253:C90–C96.

16. Pan, B.-S., and J. R. Solaro. 1987. Calcium-binding properties of troponin C in detergent-skinned heart muscle fibers. *J. Biol. Chem.* 262:7839–7849.

17. Martyn, D. A., C. J. Freitag, P. B. Chase, and A. M. Gordon. 1999. Ca2+ and crossbridge-induced changes in troponin C in skinned skeletal muscle fibers: effects of force inhibition. *Biophys. J.* 76:1480–1493.

18. Hofmann, P. A., and F. Fuchs. 1988. Bound calcium and force development in skinned cardiac muscle bundles: effect of sarcomere length. *J. Mol. Cell. Cardiol.* 20:667–677.

19. Hofmann, P. A., and F. Fuchs. 1987. Evidence for a force-dependent component of calcium binding to cardiac troponin C. *Am. J. Physiol.* 253:C541–C546.

20. Fuchs, F. 1985. The binding of calcium to detergent-extracted rabbit psoas muscle fibers during relaxation and force generation. *J. Muscle Res. Cell Motil.* 6:477–486.

21. Fuchs, F., and Y.-P. Wang. 1991. Force, length, and Ca2+-troponin C affinity in skeletal muscle. *Am. J. Physiol.* 261:C787–C792.

22. Wang, Y. P., and F. Fuchs. 1994. Length, force, and Ca(2+)-troponin C affinity in cardiac and slow skeletal muscle. *Am. J. Physiol.* 266:C1077–C1082.

23. Guth, K., and J. D. Potter. 1987. Effect of rigor and cycling cross-bridges of the structure of Troponin C and on the Ca2+ affinity of the Ca2+-specific regulatory sites in skinned rabbit psoas fibers. *J. Biol. Chem.* 262:13627–13635.

24. Allen, T. S., L. D. Yates, and A. M. Gordon. 1992. Ca2+-dependence of structural changes in troponin-C in demembranated fibers of rabbit psoas muscle. *Biophys. J.* 61:399–409.

25. Morano, I., and J. C. Ruegg. 1991. What does TnCDANZ fluorescence reveal about the thin filament state? *Pflugers Arch.* 418:333–337.

26. Martyn, D. A., and A. M. Gordon. 2001. Influence of length on force and activation-dependent changes in troponin C structure in skinned cardiac and fast skeletal muscle. *Biophys. J.* 80:2798–2808.

27. Martyn, D. A., M. Regnier, D. Xu, and A. M. Gordon. 2001. Ca2+- and cross-bridge-dependent changes in N- and C-terminal structure of troponin C in rat cardiac muscle. *Biophys. J.* 80:360–370.

28. Patel, J. R., K. S. McDonald, M. R. Wolff, and R. L. Moss. 1997. Ca2+ binding to troponin C in skinned skeletal muscle fibers assessed with caged Ca2+ and a Ca2+ fluorophore. Invariance of Ca2+ binding as a function of sarcomere length. *J. Biol. Chem.* 272:6018–6027.

29. Gordon, A., and E. Ridgway. 1987. Extra calcium on shortening in barnacle muscle. Is the decrease in calcium binding related to decreased cross-bridge attachment, force, or length? *J. Gen. Physiol.* 90:321–340.

30. Caputo, C., K. A. Edman, F. Lou, and Y. Sun. 1994. Variation in myoplasmic Ca2+ concentration during contraction and relaxation studied by the indicator fluo-3 in frog muscle fibres. *J. Physiol.* 478:137–148.

31. Wang, Y., and W. G. L. Kerrick. 2002. The off rate of Ca2+ from troponin C is regulated by force-generating cross-bridges in skeletal muscle. *J. Appl. Physiol.* 92:2409–2418.

32. Swartz, D. R., M. L. Greaser, and B. B. Marsh. 1990. Regulation of binding of subfragment 1 in isolated rigor myofibrils. *J. Cell Biol.* 111:2989–3001.

33. Maytum, R., S. S. Lehrer, and M. A. Geeves. 1999. Cooperativity and switching within the three-state model of muscle regulation. *Biochemistry.* 38:1102–1110.

34. Regnier, M., A. J. Rivera, C.-K. Wang, M. A. Bates, P. B. Chase, and A. M. Gordon. 2002. Thin filament near-neighbour regulatory unit interactions affect rabbit skeletal muscle steady-state force-Ca2+ relations. *J. Physiol.* 540:485–497.

35. Gong, H., V. Hatch, L. Ali, W. Lehman, R. Craig, and L. S. Tobacman. 2005. Mini-thin filaments regulated by troponin-tropomyosin. *Proc. Natl. Acad. Sci. USA.* 102:656–661.

36. Winegrad, S. 1965. The location of muscle calcium with respect to the myofibrils. *J. Gen. Physiol.* 48:997–1002.

37. Kitazawa, T., H. Shuman, and A. P. Somlyo. 1982. Calcium and magnesium binding to thin and thick filaments in skinned muscle fibers: electron probe analysis. *J. Muscle Res. Cell Motil.* 3:437–454.

38. Cantino, M. E., T. S. Allen, and A. M. Gordon. 1993. Subsarcomeric distribution of calcium in demembranated fibers of rabbit psoas muscle. *Biophys. J.* 64:211–222.

39. Cantino, M. E., J. G. Eichen, and S. B. Daniels. 1998. Distributions of calcium in A and I bands of skinned vertebrate muscle fibers stretched to beyond filament overlap. *Biophys. J.* 75:948–956.

40. Cantino, M. E., and J. G. Eichen. 1998. Determination of myofilament calcium distributions from electron probe x-ray microanalysis images. *Microsc. Microanal.* 4:133–140.

41. Chiu, Y., J. Asayama, and L. E. Ford. 1982. A sensitive photoelectric force transducer with a resonant frequency of 6 kHz. *Am. J. Physiol.* 243:C299–C302.

42. Hellam, D. C., and R. J. Podolsky. 1969. Force measurements in skinned muscle fibers. *J. Physiol.* 200:807–819.

43. Fabiato, A. 1988. Computer programs for calculating total from specified free or free from specified total ionic concentrations in aqueous solutions containing multiple metals and ligands. *Methods Enzymol.* 157:378–413.

44. Laemmli, U. K. 1970. Cleavage of structural proteins during assembly of head of bacteriophage-T4. *Nature.* 227:680–685.

45. Hall, T. A., and B. L. Gupta. 1982. Quantification for the x-ray microanalysis of cryosections. *J. Microsc.* 126:333–354.

46. Shuman, H., A. V. Somlyo, and A. P. Somlyo. 1976. Quantitative electron probe microanalysis of biological thin sections: methods and validity. *Ultramicroscopy.* 1:317–339.

47. Trombitas, K., M. Greaser, S. Labeit, J.-P. Jin, M. Kellermayer, M. Helmes, and H. Granzier. 1998. Titin extensibility in situ: entropic elasticity of permanently folded and permanently unfolded molecular segments. *J. Cell Biol.* 140:853–859.

48. Fuchs, F., and B. Black. 1980. The effect of magnesium ions on the binding of calcium ions to glycerinated rabbit psoas muscle fibers. *Biochim. Biophys. Acta.* 622:52–62.

49. Vandenboom, R., D. R. Claflin, and F. J. Julian. 1998. Effects of rapid shortening on rate of force regeneration and myoplasmic [Ca2+] in intact frog skeletal muscle fibres. *J. Physiol.* 511:171–180.

50. Moreno-Gonzalez, A., J. Fredlund, and M. Regnier. 2005. Cardiac troponin C (TnC) and a site I skeletal TnC mutant alter Ca2+ versus crossbridge contribution to force in rabbit skeletal fibres. *J. Physiol.* 562:873–884.

51. Huxley, H. E., A. Stewart, H. Sosa, and T. Irving. 1994. X-ray diffraction measurements of the extensibility of actin and myosin filaments in contracting muscle. *Biophys. J.* 67:2411–2421.

52. Wakabayashi, K., Y. Sugimoto, H. Tanaka, Y. Ueno, Y. Takezawa, and Y. Amemiya. 1994. X-ray diffraction evidence for the extensibility of actin and myosin filaments during muscle contraction. *Biophys. J.* 67:2422–2435.

53. Tsaturyan, A. K., N. Koubassova, M. A. Ferenczi, T. Narayanan, M. Roessle, and S. Y. Bershitsky. 2005. Strong binding of myosin heads stretches and twists the actin helix. *Biophys. J.* 88:1902–1910.

54. Cantino, M. E., and A. Quintanilla. 2002. BDM reduces enhancement of calcium bound in the overlap region of rabbit psoas muscle fibers. *Biophys. J.* 82:378a. (Abstr.).

55. Zot, H. G., and J. D. Potter. 1982. A structural role for the Ca2+-Mg2+ sites on troponin C in the regulation of muscle contraction. *J. Biol. Chem.* 257:7678–7683.

56. Finley, N. L., J. W. Howarth, and P. R. Rosevear. 2004. Structure of the Mg 2+-loaded C–lobe of cardiac troponin C bound to the N-domain of cardiac troponin I: comparison with the Ca 2+-loaded structure. *Biochemistry.* 43:11371–11379.

57. Burkart, E. M., G. M. Arteaga, M. P. Sumandea, R. Prabhakar, D. F. Wieczorek, and R. J. Solaro. 2003. Altered signaling surrounding the C-lobe of cardiac troponin C in myofilaments containing an [alpha]-tropomyosin mutation linked to familial hypertrophic cardiomyopathy. *J. Mol. Cell. Cardiol.* 35:1285–1293.

58. Tatsumi, R., K. Maeda, A. Hattori, and K. Takahashi. 2001. Calcium binding to an elastic portion of connectin/titin filaments. *J. Muscle Res. Cell Motil.* 22:149–162.

59. Labeit, D., K. Watanabe, C. Witt, H. Fujita, Y. Wu, S. Lahmers, T. Funck, S. Labeit, and H. Granzier. 2003. Calcium-dependent molecular spring elements in the giant protein titin. *Proc. Natl. Acad. Sci. USA.* 100:13716–13721.